INTERNATIONAL JOURNAL OF ELECTRICAL ENGINEERING & TECHNOLOGY (IJEET)

ISSN 0976 – 6545(Print)
ISSN 0976 – 6553(Online)
Volume 6, Issue 3, March (2015), pp. 17-31
© IAEME: www.iaeme.com/IJEET.asp
Journal Impact Factor (2015): 7.7385 (Calculated by GISI)
www.jifactor.com

IJEET

©IAEME

COMPARATIVE ANALYSIS OF APPROXIMATE AND DYNAMIC MODEL OF FIVE PHASE INDUCTION MOTOR

Mitesh B. Astik

A.D. Patel Institute of Technology, New V.V. Nagar, Anand, Gujarat, India

ABSTRACT

In this paper, an approximate and dynamic modeling of five-phase induction motor is described in a step by step approach. A dq model based on transformation theory for five-phase induction machine is presented. A detailed implementation of an indirect-type five-phase field oriented control including the hysteresis-type pulse width modulation (PWM) current regulator is described for both approximate as well as for dynamic model. Simulations have been carried out for different load conditions. Simulation results verify that the performance of dynamic model is superior to approximate model.

Index: Approximate Model, Dynamic Model, Five-Phase Induction Motor, Indirect Vector Control.

1. INTRODUCTION

The five-phase machines are found to possess several advantages over three-phase machines such as an increase in current per phase without the need to increase the phase voltage, reduction in amplitude and increase in frequency of pulsating torques, fault tolerance, stability and lower current ripple [1]. Another important aspect of machines with a higher number of phases is their improved reliability, since they can operate even when one or two phases are missing. It has also been shown that increasing the number of phases can result in an increase in the torque/ampere relation for the same volume machines [2]-[4]. Hence the analysis, design and application of machines with high phase numbers require adequate mathematical models to be established, through which their performance and advantages can be assessed.

In this paper, comparison of an approximate model from the equivalent circuit of five-phase induction motor which is presented in [5] and a dynamic model of five-phase induction motor is described. Simulink induction machine models are available in the literature [6]-[7], but they appear to be black-boxes with no internal details. In this paper each block solves one of the model equations.

In this paper, the necessary differential equations describing the performance of five-phase induction machines in d-q frame of reference based on transformation theory are presented for both approximate and dynamic model. A detailed implementation of an indirect-type five-phase field-orientation control including the hysteresis type of PWM current regulator is illustrated [8]. Simulations have been carried out for different load conditions.

2. APPROXIMATE MODELING OF FIVE-PHASE INDUCTION-MOTOR

Our goal is to transform the five-phase stationary reference frame (as-bs-cs-ds-es) variables into two-phase stationary reference frame (ds-qs) variables. Five-phase voltages and currents can be transformed into two-phase voltages and currents using (1) and (2) respectively.

$$\begin{bmatrix} V_{ds} \\ V_{qs} \\ V_{ns} \end{bmatrix} = \frac{2}{5} \begin{pmatrix} \cos\theta & \cos(\theta - 2\Pi/5) & \cos(\theta - 4\Pi/5) & \cos(\theta + 4\Pi/5) & \cos(\theta + 2\Pi/5) \\ \sin\theta & \sin(\theta - 2\Pi/5) & \sin(\theta - 4\Pi/5) & \sin(\theta + 4\Pi/5) & \sin(\theta + 2\Pi/5) \\ \frac{1}{\sqrt{2}} & \frac{1}{\sqrt{2}} & \frac{1}{\sqrt{2}} & \frac{1}{\sqrt{2}} & \frac{1}{\sqrt{2}} \end{pmatrix} \begin{bmatrix} V_{as} \\ V_{bs} \\ V_{cs} \\ V_{ds} \\ V_{es} \end{bmatrix} \quad (1)$$

$$\begin{bmatrix} I_{ds} \\ I_{qs} \\ I_{ns} \end{bmatrix} = \frac{2}{5} \begin{pmatrix} \cos\theta & \cos(\theta - 2\Pi/5) & \cos(\theta - 4\Pi/5) & \cos(\theta + 4\Pi/5) & \cos(\theta + 2\Pi/5) \\ \sin\theta & \sin(\theta - 2\Pi/5) & \sin(\theta - 4\Pi/5) & \sin(\theta + 4\Pi/5) & \sin(\theta + 2\Pi/5) \\ \frac{1}{\sqrt{2}} & \frac{1}{\sqrt{2}} & \frac{1}{\sqrt{2}} & \frac{1}{\sqrt{2}} & \frac{1}{\sqrt{2}} \end{pmatrix} \begin{bmatrix} I_{as} \\ I_{bs} \\ I_{cs} \\ I_{ds} \\ I_{es} \end{bmatrix} \quad (2)$$

where, V_{as}, V_{bs}, V_{cs}, V_{ds} and V_{es} are stator phase voltages. V_{ds} and V_{qs} are the d^s and q^s axis stator fundamental voltages respectively. V_{ns} is the zero sequence component of the stator. It is convenient to set $\theta = 0$, so that the q^s axis is aligned with the as-axis. Ignoring the zero sequence components, the transformation relations can be simplified using (3)-(4).

$$V_{qs} = \frac{2}{5}\left[V_a + V_b \cos(-2\Pi/5) + V_c \cos(-4\Pi/5) + V_d \cos(4\Pi/5) + V_e \cos(2\Pi/5)\right] \quad (3)$$

$$V_{ds} = \frac{2}{5}\left[V_b \sin(-2\Pi/5) + V_c \sin(-4\Pi/5) + V_d \sin(4\Pi/5) + V_e \sin(2\Pi/5)\right] \quad (4)$$

The Electro Motive Forces (EMFs) induced in rotor d and q axes are

$$E_{dr} = V_{ds} * K, \; E_{qr} = V_{qs} * K \quad (5)$$

where
$$K = \frac{T_r\,(rotor\ turns)}{T_s\ (stator\ turns)} \quad (6)$$

The impedance of rotor winding is given by

$$Z_2 = \sqrt{\left(R_2/s\right)^2 + (X_2)^2} \tag{7}$$

where R_2, X_2 and Z_2 are rotor resistor, reactance and impedance respectively.
The currents produced in rotor d and q axis are

$$I_{dr} = \frac{E_{dr}}{Z_2} \quad ; \qquad I_{qr} = \frac{E_{qr}}{Z_2} \tag{8}$$

Now, rotor currents with respect to stator are

$$I_{dr}' = I_{dr} * K \quad ; \quad I_{qr}' = I_{qr} * K \tag{9}$$

Magnetizing impedance of motor is given by

$$Z_0 = \sqrt{(R_0)^2 + (X_0)^2} \tag{10}$$

where, R_0 is non-inductive resistance and X_0 is magnetizing reactance.
d and q axes stator magnetizing currents are given by

$$I_{ds} = \sqrt{(I_{dr})^2 + (I_{ds0})^2} \; ; I_{qs} = \sqrt{(I_{qr})^2 + (I_{qs0})^2} \tag{11}$$

$$\text{where, } I_{ds0} = V_{ds}/Z_0 \quad ; \quad I_{qs0} = V_{qs}/Z_0 \tag{12}$$

Fig. 1 shows the block diagram of approximate model dq currents.

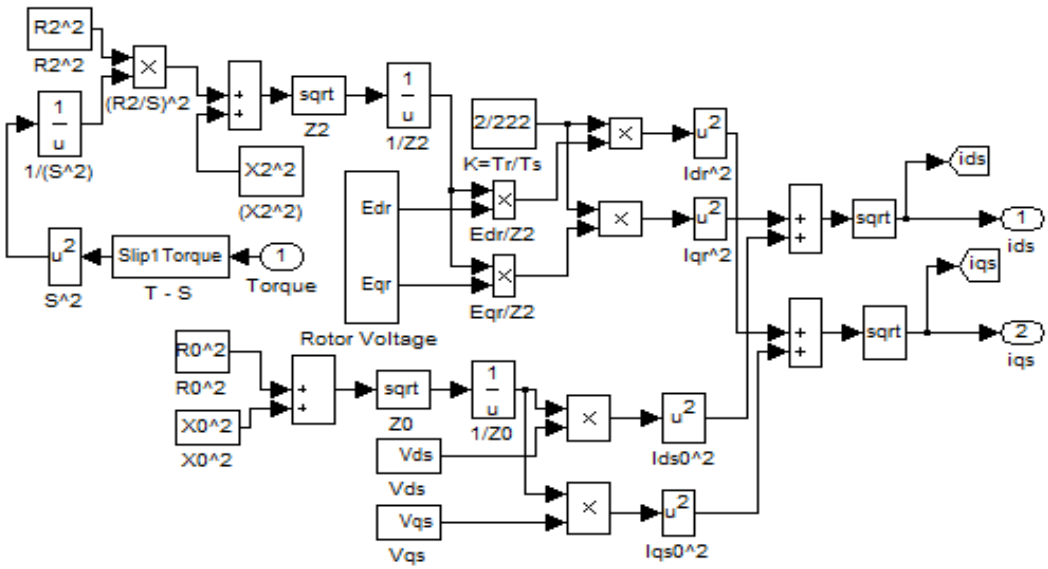

Fig. 1 Block diagram of approximate model dq currents

Torque produce in five-phase induction motor is given by

$$T_e = \frac{5}{2}\frac{P}{2}\left(L_{md}\, i_{qs} - L_{mq}\, i_{ds}\right) \quad (13)$$

where P is the number of poles, L_{md} and L_{mq} are the d and q axis mutual inductance respectively.

Now, the angular speed of the motor is given by $\omega = \int \frac{T_e - T_L}{J} dt$ (14)

where ω is mechanical speed of the motor, T_e is the electromechanical torque and T_L is load torque and J is moment of inertia.

$$s = (\omega_s - \omega) / \omega_s \quad (15)$$

where s is slip of the motor and ω_s is the synchronous speed of the motor. Fig. 2 shows the approximate model torque-slip block diagram.

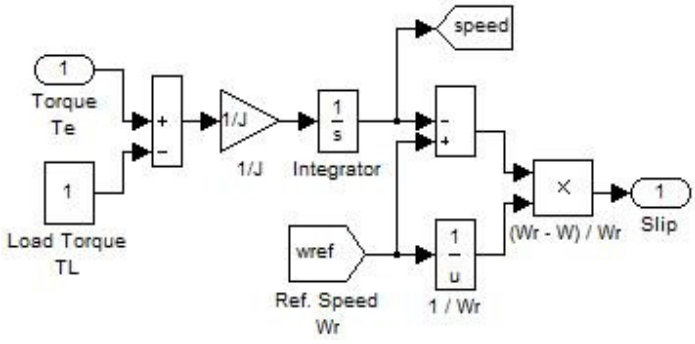

Fig. 2 Approximate model Torque-Slip block diagram

3. DYNAMIC MODELING OF FIVE-PHASE INDUCTION MOTOR

The five-phase stationary reference frame (as-bs-cs-ds-es) variables are transformed into two-phase stationary reference frame (d^s-q^s) variables and then transform these variables into synchronously rotating reference frame (d^e-q^e) and vice-versa. The voltage as-bs-cs-ds-es can be resolved into V_{ds} and V_{qs} components and can be represented in the matrix form using (1).

Using (3)-(4), we can find the dq axis voltage. The two-phase d^s-q^s winding are transformed into the hypothetical windings mounted on the d^e-q^e axis, which rotate at synchronous speed ω_e with respect to the d^s-q^s axis and the angle $\theta_e = \omega_e t$. the voltage on the d^s-q^s axis can be converted into the d^e-q^e frame as follows[9]-[10]:

$$\begin{bmatrix} V_{qe} \\ V_{de} \end{bmatrix} = \begin{bmatrix} \cos\theta & -\sin\theta \\ \sin\theta & \cos\theta \end{bmatrix} \begin{bmatrix} V_{qs} \\ V_{ds} \end{bmatrix} \quad (16)$$

For the two-phase machine, we need to represent both d^s-q^s and d^r-q^r circuit and their variables in a synchronously rotating d^e-q^e frame. The d^e-q^e frame voltage expressions are:

$$V_{qs} = R_s\, i_{qs} + \frac{d}{dt}\Psi_{qs} + \omega_e\, \Psi_{ds} \quad (17)$$

$$V_{ds} = R_s\, i_{ds} + \frac{d}{dt}\Psi_{ds} - \omega_e\, \Psi_{qs} \quad (18)$$

$$V_{qr} = R_r\, i_{qr} + \frac{d}{dt}\Psi_{qr} - \omega_e\, \Psi_{dr} \quad (19)$$

$$V_{dr} = R_r\, i_{dr} + \frac{d}{dt}\Psi_{dr} - \omega_e\, \Psi_{qr} \quad (20)$$

Since the rotor actually moves at speed ω_r, the dq axes fixed on the rotor which moves at a speed of $(\omega_e - \omega_r)$ relative to the synchronously rotating frame. The flux linkage expressions for dq frame are:

$$F_{qs} = \omega_b\, \Psi_{qs} = X_{ls}\, i_{qs} + X_m\, (i_{qs} + i_{qr}) \quad (21)$$

$$F_{qr} = \omega_b\, \Psi_{qr} = X_{lr}\, i_{qr} + X_m\, (i_{qs} + i_{qr}) \quad (22)$$

$$F_{ds} = \omega_b\, \Psi_{ds} = X_{ls}\, i_{ds} + X_m\, (i_{ds} + i_{dr}) \quad (23)$$

$$F_{dr} = \omega_b\, \Psi_{dr} = X_{lr}\, i_{dr} + X_m\, (i_{ds} + i_{dr}) \quad (24)$$

$$F_{qm} = \omega_b\, \Psi_{qm} = X_m\, (i_{qs} + i_{qr}) \quad (25)$$

$$F_{dm} = \omega_b\, \Psi_{dm} = X_m\, (i_{ds} + i_{dr}) \quad (26)$$

where $X_{ls} = \omega_b\, L_{ls}$, $X_{lr} = \omega_b\, L_{lr}$ and $X_m = \omega_b\, L_m$ (27)

By substituting (21)-(24) in (17)-(20), the voltage expressions can be written as:

$$V_{qs} = R_s\, i_{qs} + \frac{1}{\omega_b}\frac{d}{dt}F_{qs} + \frac{\omega_e}{\omega_b}F_{ds} \quad (28)$$

$$V_{ds} = R_s\, i_{ds} + \frac{1}{\omega_b}\frac{d}{dt}F_{ds} - \frac{\omega_e}{\omega_b}F_{qs} \quad (29)$$

$$0 = R_r\, i_{qr} + \frac{1}{\omega_b}\frac{d}{dt}F_{qr} + \frac{(\omega_e - \omega_r)}{\omega_b}F_{dr} \quad (30)$$

$$0 = R_r\, i_{dr} + \frac{1}{\omega_b}\frac{d}{dt}F_{dr} - \frac{(\omega_e - \omega_r)}{\omega_b}F_{qr} \quad (31)$$

By substituting (27) in (21)-(24), the flux linkage equations can be written as

$$\frac{F_{qs}}{\omega_b} = \left[(L_{ls} + L_m)\, i_{qs} + L_m\, i_{qr}\right] \quad (32)$$

$$\frac{F_{ds}}{\omega_b} = \left[(L_{ls} + L_m)\, i_{ds} + L_m\, i_{dr}\right] \quad (33)$$

$$\frac{F_{qr}}{\omega_b} = \left[(L_{lr} + L_m)\, i_{qr} + L_m\, i_{qs}\right] \quad (34)$$

$$\frac{F_{dr}}{\omega_b} = \left[(L_{lr} + L_m)\, i_{dr} + L_m\, i_{ds}\right] \quad (35)$$

By substituting (32)-(33) in (28), we get (36)-(37).

$$\frac{d\,(L_{ls} + L_m)\, i_{qs}}{dt} = V_{qs} - L_m\frac{d\, i_{qr}}{dt} - R_s\, i_{qs} - \omega_e\left[(L_{ls} + L_m)\, i_{ds} + L_m\, i_{dr}\right] \quad (36)$$

$$i_{qs} = \int \frac{1}{(L_{ls} + L_m)} \left\{ V_{qs} - L_m \frac{d\, i_{qr}}{dt} - R_s\, i_{qs} - \omega_e \left[(L_{ls} + L_m)\, i_{ds} + L_m\, i_{dr} \right] \right\} \quad (37)$$

Similarly, we can write remaining current equations as given in (38)-(40).

$$i_{ds} = \int \frac{1}{(L_{ls} + L_m)} \left\{ V_{ds} - L_m \frac{d\, i_{dr}}{dt} - R_s\, i_{ds} + \omega_e \left[(L_{ls} + L_m)\, i_{qs} + L_m\, i_{qr} \right] \right\} \quad (38)$$

$$i_{qr} = \int \frac{1}{(L_{lr} + L_m)} \left\{ - L_m \frac{d\, i_{qs}}{dt} - R_r\, i_{qr} - (\omega_e - \omega_r) \left[(L_{lr} + L_m)\, i_{dr} + L_m\, i_{ds} \right] \right\} \quad (39)$$

$$i_{dr} = \int \frac{1}{(L_{lr} + L_m)} \left\{ - L_m \frac{d\, i_{ds}}{dt} - R_r\, i_{dr} + (\omega_e - \omega_r) \left[(L_{lr} + L_m)\, i_{qr} + L_m\, i_{qs} \right] \right\} \quad (40)$$

The simulation block diagram of q-axis stator current is shown in Fig. 3 which can be done using (37).

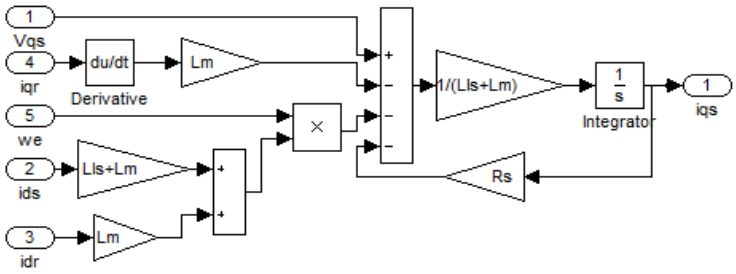

Fig. 3 Simulink implementation for i_{qs}

Similarly, we can simulate the remaining current expressions i.e. i_{ds}, i_{qr} and i_{dr} using (38)-(40) respectively. Now, the flux linkage expressions in terms of currents can be written as follows:

$$\Psi_{qs} = L_{ls}\, i_{qs} + L_m\, (i_{qs} + i_{qr}) \quad (41)$$

$$\Psi_{ds} = L_{ls}\, i_{ds} + L_m\, (i_{ds} + i_{dr}) \quad (42)$$

$$\Psi_{qr} = L_{lr}\, i_{qr} + L_m\, (i_{qs} + i_{qr}) \quad (43)$$

$$\Psi_{dr} = L_{lr}\, i_{dr} + L_m\, (i_{ds} + i_{dr}) \quad (44)$$

$$\Psi_{qm} = L_m\, (i_{qs} + i_{qr}) \quad (45)$$

$$\Psi_{dm} = L_m\, (i_{ds} + i_{dr}) \quad (46)$$

The simulation block for q-axis stator flux linkage is shown in Fig. 4 which can be done using (41). Similarly, we can simulate the remaining flux linkage expressions i.e. Ψ_{ds}, Ψ_{qr} and Ψ_{dr} using (42)-(44) respectively.

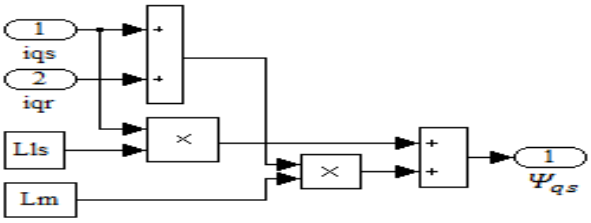

Fig. 4 Simulink implementation for Ψ_{qs}

The simulation of dq-axis mutual flux linkage is shown in Fig. 5 using (45)-(46).

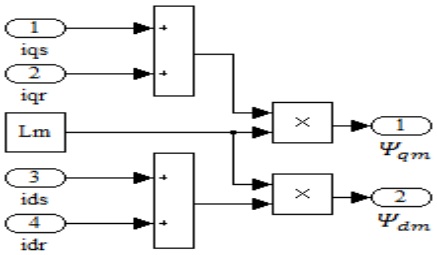

Fig. 5 Simulink implementation for Ψ_{qm} and Ψ_{dm}

Now, the torque expression can be written as follows:

$$T_e = \frac{5}{2}\frac{P}{2}\frac{L_m}{(L_m + L_{lr})}(\Psi_{dr}\, i_{qs} - \Psi_{qr}\, i_{ds}) \quad (47)$$

The speed and torque are given by the following relation:

$$J\frac{d\,\omega_r}{dt} + B\,\omega_r = T_e - T_L \quad (48)$$

The torque and speed equations can be simulate from (47)-(48) which is shown in Fig. 6.

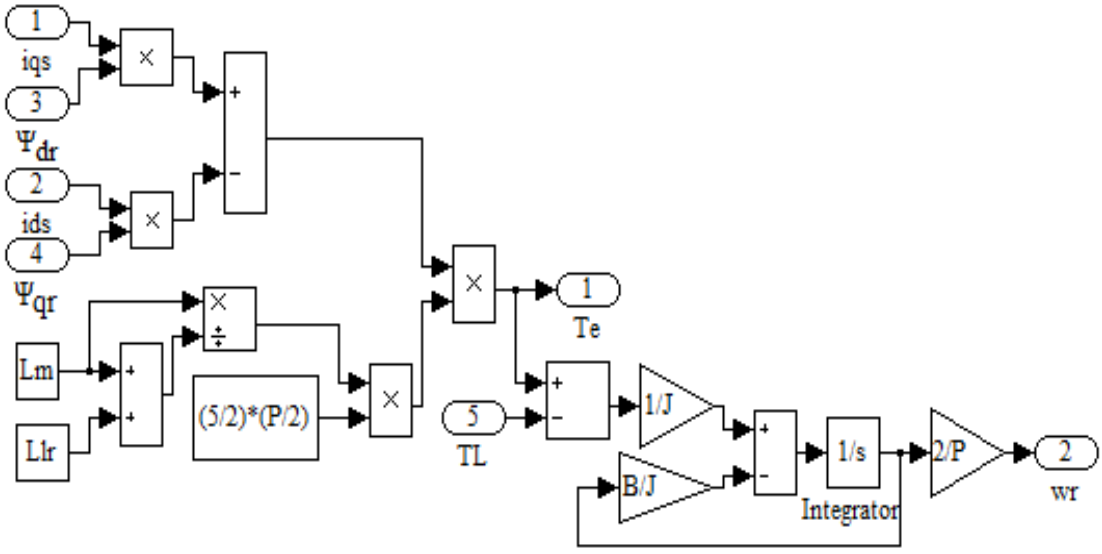

Fig. 6 Simulink implementation for Torque and Speed

International Journal of Electrical Engineering and Technology (IJEET), ISSN 0976 – 6545(Print), ISSN 0976 – 6553(Online) Volume 6, Issue 3, March (2015), pp. 17-31 © IAEME

4. CONTROLLER OF FIVE-PHASE INDUCTION-MOTOR (INDIRECT VECTOR CONTROL METHOD)

Fig. 7 shows the complete block diagram of indirect vector control method.

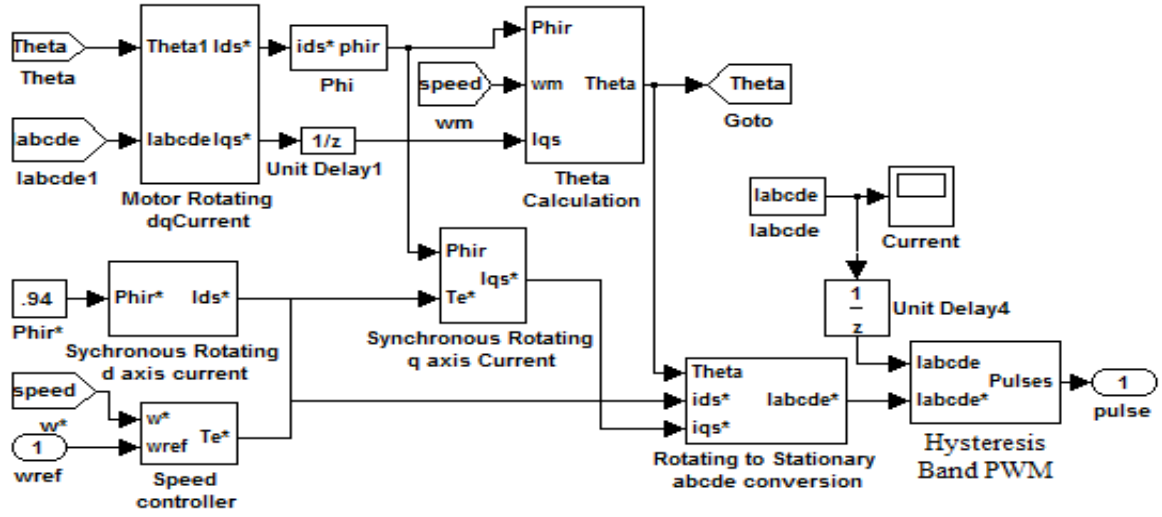

Fig. 7 Total Block diagram of indirect vector control Method

4.1 dq axis rotating current

The five-phase currents can be resolved into i_{ds} and i_{qs} components and can be represented in the matrix form from (2). Simulation of dq-axis rotating currents is shown in Fig. 8.

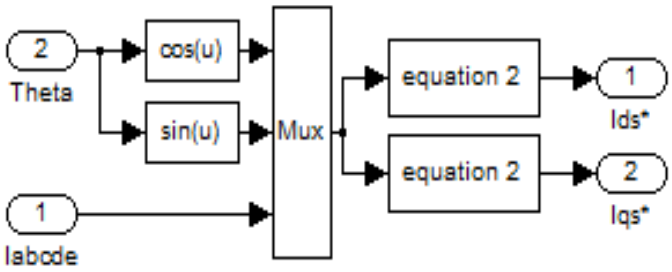

Fig. 8 Simulink implementation for d-q axis rotating currents

4.2 Flux Phir

The flux produced in the stator winding is given by

$$Phir = \frac{L_m I_{ds}^*}{(1 + T s)} \tag{49}$$

where $T = L_r / R_r$. The simulation block of flux phir is shown in Fig. 9.

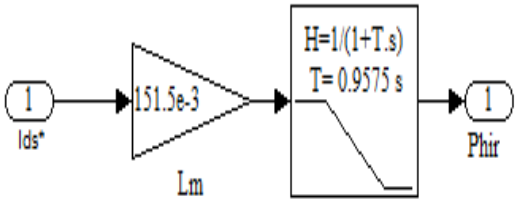

Fig. 9 Simulink implementation for flux Phir

4.3 Rotor position

Now, the rotor position $\theta = \int (\omega_r + \omega_m)$ (50)

where, ω_m mechanical speed and ω_r is rotor frequency (rad/sec)

$$\omega_r = \frac{L_m \, i_{qs} \, R_r}{(L_r * Phir)} \quad (51)$$

The block diagram of rotor position theta can be simulate as shown in Fig. 10.

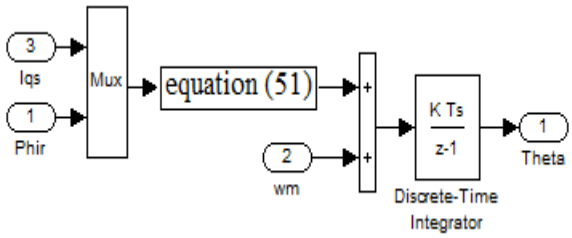

Fig. 10 Simulink implementation for Theta

4.4 Fundamental reference torque (T_e*)

The fundamental reference torque (T_e*) shown in Fig. 11 is obtained by using proportional plus integral (PI) controller whose input is the error between the actual and reference speed.

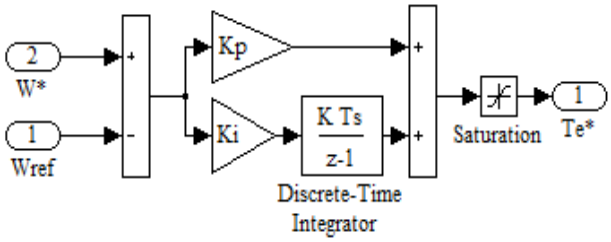

Fig. 11 Simulink implementation for fundamental reference torque (T_e*)

4.5 Synchronous rotating dq-axis current

The dq-axis synchronous rotating currents are given by

$$i_{ds}^{*} = \frac{Phir^{*}}{L_{md}} \quad (52)$$

$$i_{qs}^{*} = \frac{2}{5}\frac{2}{P}\frac{L_r}{L_{mq}}\frac{T_e^{*}}{Phir} \quad (53)$$

where phir* is constant flux, i_{ds}^{*} and i_{qs}^{*} are d and q axis synchronous rotating reference currents respectively.

4.6 Rotating to stationary abcde conversion

Now, the rotating currents are transformed into stationary five-phase currents (i_{abcde}*) by taking inverse of (2).

4.7 Hysteresis Control PWM

With the use of hysteresis control PWM method, actual and reference five-phase currents are compared and the gate pulses are generated to control the five-phase induction motor [5]. Fig. 12 shows the block diagram of hysteresis control PWM.

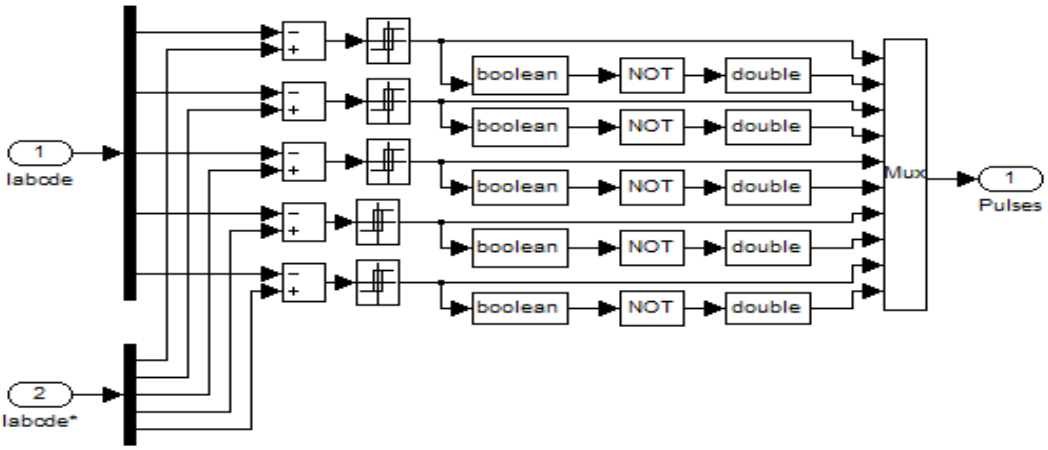

Fig. 12 Block diagram of Hysteresis Control PWM

Fig. 13 shows the simulation of five-phase voltages from the gate pulses. These five-phase voltages applied to the five-phase induction motor.

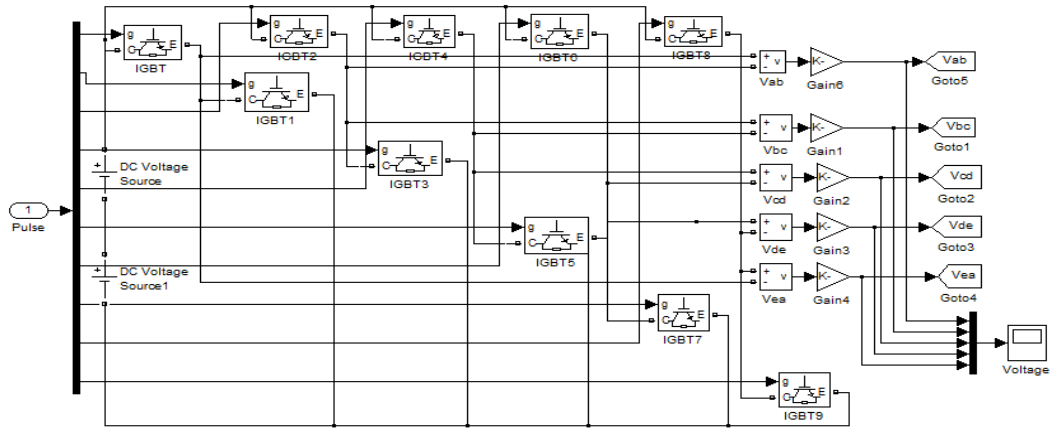

Fig. 13 Five-phase voltage from the gate pulses

5. SIMULATION RESULTS

Fig. 14(a) and (b) show the simulation result of no-load speed of approximate and dynamic model respectively.

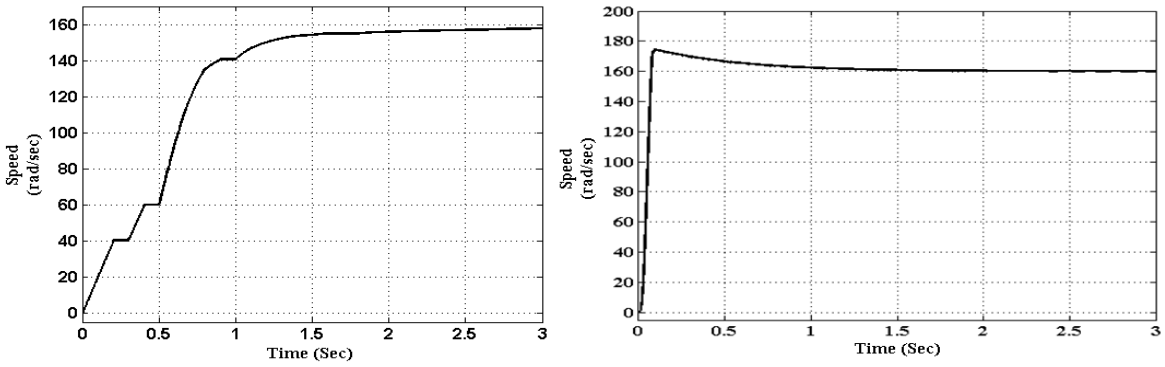

(a) **(b)**

Fig. 14 No-Load Speed (a) Approximate Model (b) Dynamic Model

Fig. 15 (a) and (b) show the simulation result of approximate and dynamic model speed at load torque T_L = 1 Nm and T_L = 5 Nm respectively. Fig. 15 (c) and (d) show the simulation result of approximate and dynamic model speed at load torque T_L = 1 Nm and T_L = 5 Nm respectively.

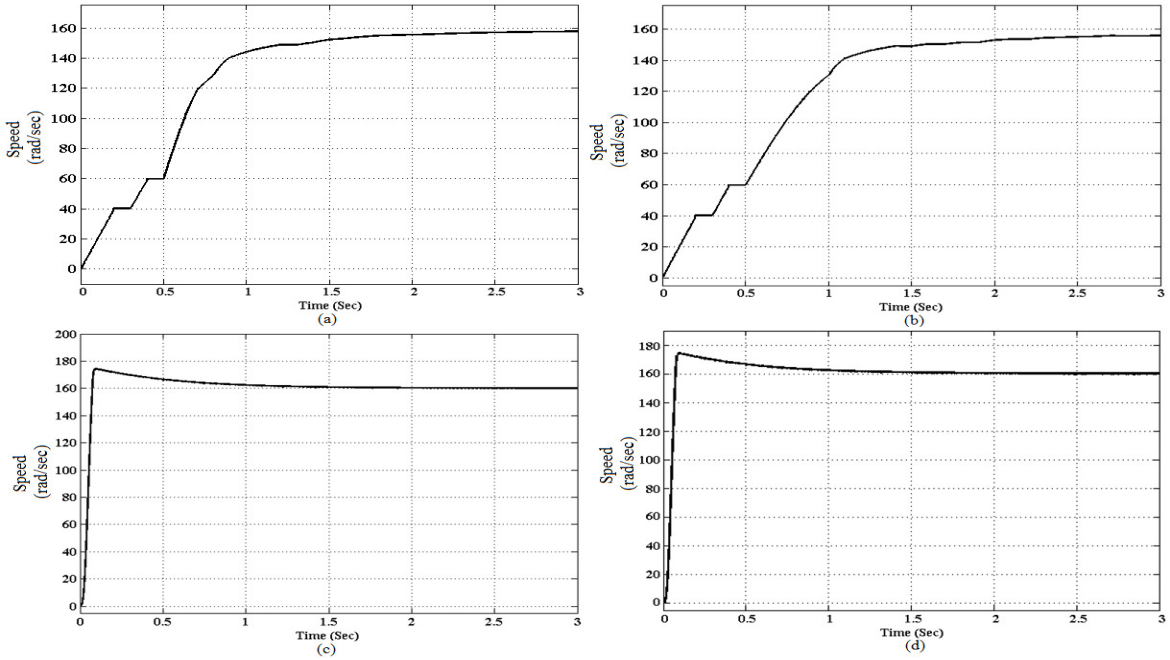

Fig. 15 Speed response (a) approximate Model at T_L = 1 Nm (b) approximate model at T_L = 5 Nm (c) dynamic model at T_L = 1 Nm (d) dynamic model at T_L = 5 Nm

Fig. 16(a) and (b) show the simulation result of no-load torque of approximate and dynamic model respectively.

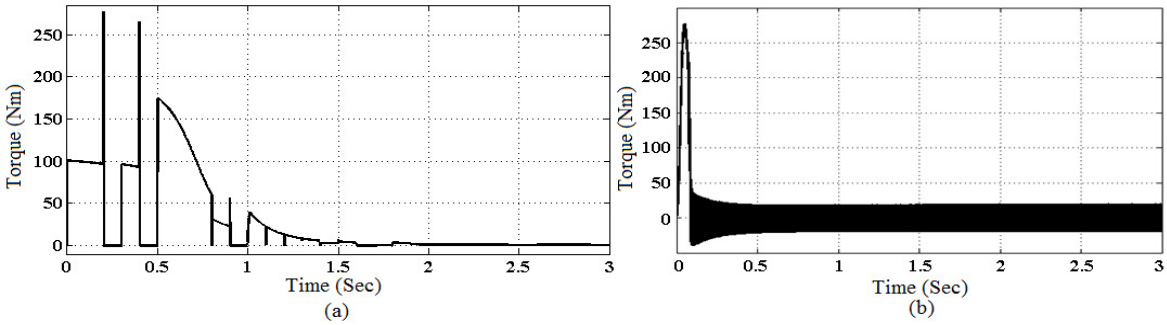

Fig. 16 No-load torque (a) approximate model (b) dynamic model

Fig. 17 (a) and (b) show the simulation result of approximate and dynamic model torque response at load torque T_L = 1 Nm and T_L = 5 Nm respectively. Fig. 17 (c) and (d) show the simulation result of approximate and dynamic model torque response at load torque T_L = 1 Nm and T_L = 5 Nm respectively.

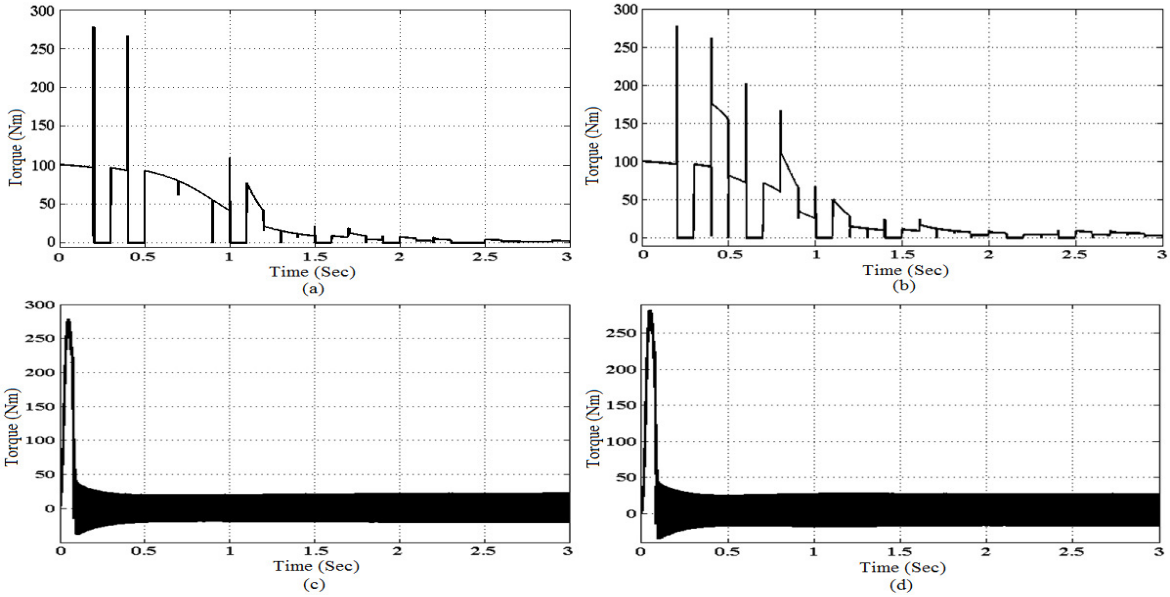

Fig. 17 Torque response (a) approximate Model at T_L = 1 Nm (b) approximate model at T_L = 5 Nm (c) dynamic model at T_L = 1 Nm (d) dynamic model at T_L = 5 Nm

Fig. 18 (a) and (b) show the simulation result of no-load current of approximate and dynamic model respectively.

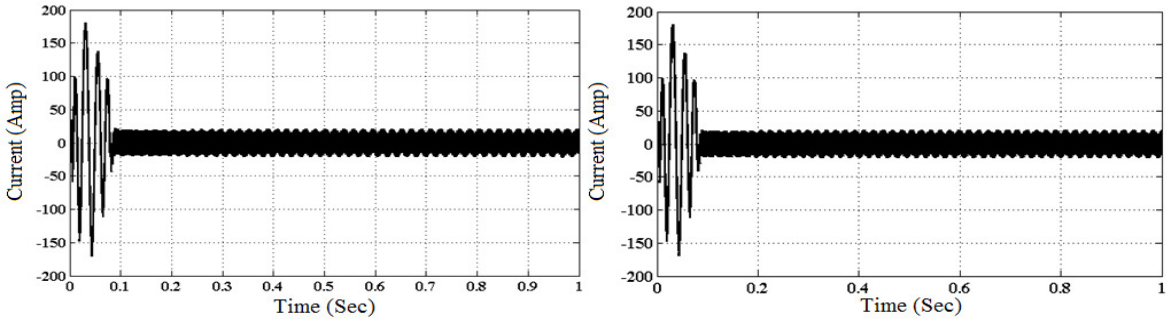

Fig. 18 No-load current (a) approximate model (b) dynamic model

Fig. 19 (a) and (b) show the simulation result of approximate and dynamic model current response at load torque T_L = 1 N-m and T_L = 5 Nm respectively. Fig. 19 (c) and (d) show the simulation result of approximate and dynamic model current response at load torque T_L = 1 N-m and T_L = 5 Nm respectively.

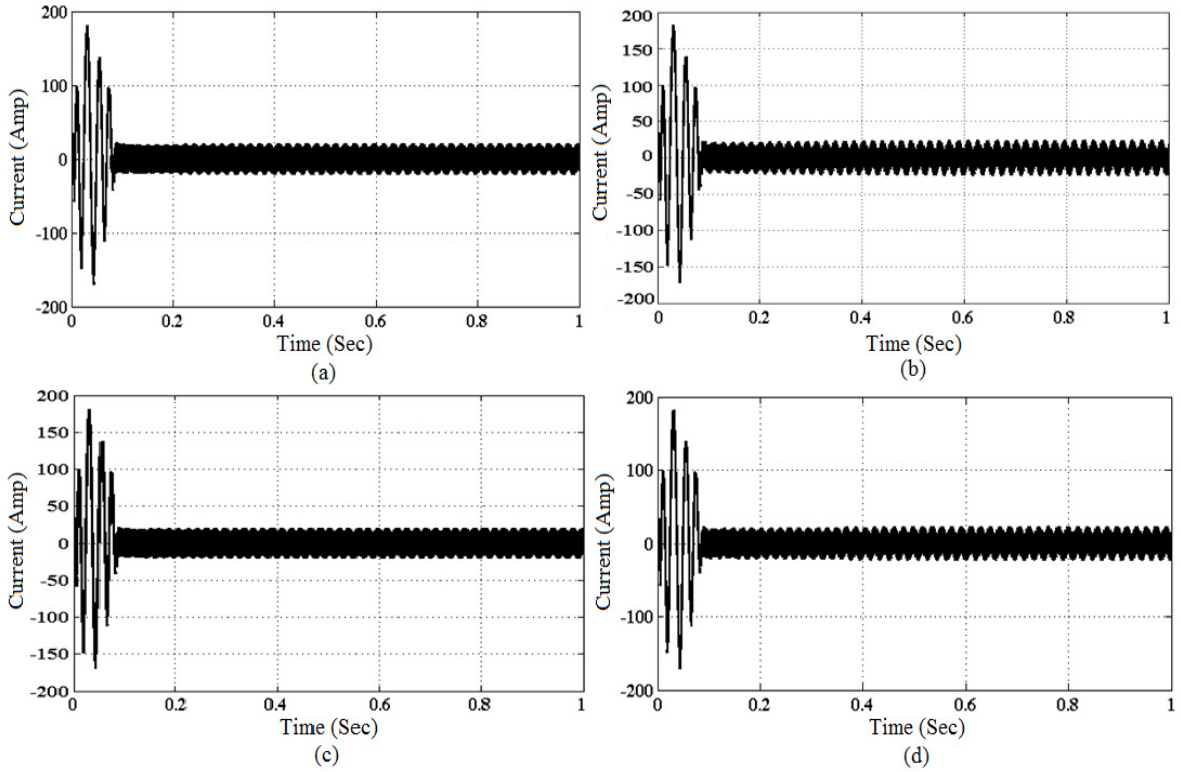

Fig. 19 Current response (a) approximate Model at T_L = 1 Nm (b) approximate model at T_L = 5 Nm (c) dynamic model at T_L = 1 Nm (d) dynamic model at T_L = 5 Nm

Table-I The comparative simulation results

Load (N-m)	Approximate Model			Dynamic Model		
	Speed (rad/sec)	Maximum Torque (Nm)	Transient Current (A)	Speed (rad/sec)	Maximum Torque (Nm)	Transient Current (A)
T_L = 0	159.8	277.64	181.72	160.00	277.84	180.52
T_L = 1	158.35	277.82	181.72	160.00	278.74	180.79
T_L = 5	157.41	278.37	183.63	160.00	282.20	182.01

It is observed from Table-I that when the motor is at no-load, the speed of approximate model is 159.8 rad/sec and the speed response is over damped. At Load torque T_L = 1 Nm, the speed of the approximate model is 158.35 rad/sec. At load torque T_L = 5 Nm, the speed of approximate model is 157.41 rad/sec. While the speed of dynamic model is 160 rad/sec for the entire load and the response of the motor is under damped. Maximum no-load torque for both the models is approximate equal. Maximum torque of approximate model torque is almost same for entire load while the maximum torque of dynamic model is gradually increased with increasing the load. Transient as well as steady state Current response of both the model are approximate similar.

6. CONCLUSION

The speed of five-phase induction motor can be controlled using different types of methods such as V/ f method, vector control method etc. Approximation and dynamic modeling and simulation of five-phase induction motor are done in this paper. The speed control of the five-phase induction motor is achieved by indirect vector control method for both the model. From the simulation result, we can see that approximate model has around 2% speed error in steady state as compared to dynamic model steady state speed. Torque produced in dynamic model is slightly more as compared to that of the approximate model. We can see the minor current difference in both the model. From the results, we can conclude that overall behavior of the dynamic model is superior to the approximate model.

APPENDIX

TABLE II parameters of five-phase induction motor

Power	7.5 hp
Voltage	400 Volt
Poles	4
Frequency	50 Hz
Stator Resistance	0.22 Ω
Rotor Resistance	0.16
Magnetizing resistance	300 Ω
Magnetizing reactance	4500 Ω
Stator leakage inductance	4.76 mH
Rotor leakage inductance	1.7 mH
Mutual inductance	151.5 mH
Mechanical motion inertia	0.04 Kg-m^2
Number of stator turns per phase	222
Number of rotor turns per phase	2

REFERENCES

1. H. Xu, H.A. Toliyat and L.J. Peterson, Modeling and Control of Five-Phase Induction Motor under Asymmetrical Fault Conditions, Proceedings of the Third Naval Symposium on Electric Machines, Philadelphia, 2000, 4-7.
2. H.A. Toliyat, Analysis and Simulation of Five-phase Variable Speed Induction-Motor Drives under Asymmetrical Connections, IEEE Transaction on Power Electronics, 13(4), 1998, 748-756.
3. H.A. Toliyat, T.A. Lipo, and J.C. White, Analysis of a concentrated winding Induction Machine for adjustable Speed Drive Application-part I (Motor Analysis), IEEE Transaction on Energy Conversion, 6(4), 1991, 679-683.
4. H.A. Toliyat, T.A. Lipo, and J.C. White, Analysis of a concentrated winding Induction Machine for adjustable Speed Drive Application-part II (Motor Design and Performance), IEEE Transaction on Energy Conversion, 6(4), 1991, 684- 692.
5. M.B. Astik and D.R. Mehta, dq Modeling and Control of Five-phase Induction Motor under Asymmetrical Connections using MATLAB Simulation, NUCONE – 2007, Nirma University, 2007, 13-17.

6. Atif Iqbal, Sk Moin Ahmed, Md Arif Khan, Mohd. Rizwan Khan and Haitham Abu-Rub, Modeling, Simulation and Implementation of a Five-Phase Induction Motor Drive System, Joint International Conference on Power Electronics, Drives and Energy Systems (PEDES-2010), Power India, 2010, 1-6.
7. Lu´is Alberto Pereira, C´esar Cataldo Scharlau, Lu´is Fernando Alves Pereira, and Jos´e Felipe Haffner, General Model of a Five-Phase Induction Machine Allowing for harmonics in the Air Gap Field, IEEE Transaction on Energy Conversion, 21(4), 2006, 891-899.
8. Burak Ozpineci and Leon M. Tolbert, Simulink Implementation of Induction Machine Model – A Modular Approach, Electric Machines and Drives Conference, IEMDC'03. IEEE International, 2, 728-734.
9. B.K. Bose, *Modern Power Electronics and AC Drives*, (Pearson Education Pvt. Ltd., Delhi, India, 3rd edition, 2003).
10. Chee-Mun Ong, *Dynamic Simulation of Electric Machinery Using Matlab/Simulink*, (Prentice Hall PTR, New Jersey, 1998).